



## Study of tetracycline and metronidazole adsorption on biochar prepared from rice bran kinetics, isotherms and mechanisms

Fatemeh Asgharzadeh<sup>a</sup>, Mitra Gholami<sup>b,c</sup>, Ahmad Jonidi<sup>b,c</sup>, Majid Kermani<sup>b,c</sup>, Hosseinali Asgharnia<sup>d</sup>, Roshanak Rezaeikalantary<sup>b,c,\*</sup>

<sup>a</sup>Department of Environmental Health Engineering, School of Public Health, International Campus, Iran University of Medical Sciences, Tehran, Iran, email: asgharzadeh.59@gmail.com (A. Fatemeh)

<sup>b</sup>Research Center for Environmental Health Technology (RCEHT), Iran University of Medical Sciences, Tehran, Iran, email: gholamimitra32@gmail.com (M. Gholami), ahmad\_jonidi@yahoo.com (A. Jonidi), majidkermani@yahoo.com (M. Kermani)

<sup>c</sup>Department of Environmental Health Engineering, School of Public Health, Iran University of Medical Sciences, Tehran, Iran, Tel. +98 9123234586, email: rezaei.k.r2016@gmail.com (R.R. Kalantari)

<sup>d</sup>Department of Environmental Health Engineering, School of Public Health, Babol University of Medical Sciences, Babol, Iran, email: ehaamin2@gmail.com (H. Asgharnia)

Received 23 November 2018; Accepted 20 March 2019

### ABSTRACT

A rice bran derived biochar was prepared at temperature of 700°C for 2 h using the pyrolysis method; the biochar was used as an adsorbent for tetracycline and metronidazole elimination. Biochar properties were determined by SEM, EDX, FT-IR and BET analyses. The batch adsorption studies were performed at different pH (3–11), adsorbent concentrations (0.25–4 g L<sup>-1</sup>), antibiotic concentrations (10–40 mg L<sup>-1</sup>), contact time (5–120 min), and temperatures (293, 298, 308, 318 K). Tetracycline and metronidazole elimination efficiency was 70% and 90%, respectively, at the biochar concentration of 1.5 g L<sup>-1</sup>, antibiotic concentrations of 10 mg L<sup>-1</sup> and a solution temperature of 298 K. The kinetic data were analyzed using two pseudo first-order and second-order models. The equilibrium data were analyzed using Langmuir and Freundlich isotherms and the results showed that the process followed the Freundlich model. The maximum adsorption capacity for tetracycline and metronidazole were 13.33 and 21.33 mg/g, respectively. The calculated values of  $\Delta G^0$  and  $\Delta H^0$  represent spontaneous and endothermic adsorption process in the studied temperature range. Thermodynamic studies also indicated the adsorption of a physical type. The effective removal of metronidazole was more than tetracycline, due to its size and electron density. The results showed that the biochar prepared in this study can be used as an alternative to expensive adsorbents for the elimination these antibiotics from aqueous solutions.

**Keywords:** Biochar; Rice bran; Metronidazole; Tetracycline; Adsorption

### 1. Introduction

Pharmaceutical compounds such as hormones, antibiotics, and heart medications are discharged into sewage systems through hospitals, commercial and residential areas, and medical and veterinary clinics [1]. The presence of antibiotics in water resources due to its high solubility in

water, low degradability and high toxicity is a serious threat to the environment and human health [2]. The major reason for antibiotic excretion into the environment is inadequate absorption of medications by human beings and feedlot animals; also, conventional treatment processes can only remove 60–90% of antibiotics [2–4]. Therefore, it is imperative that antibiotics be treated completely [3]. Antibacterial materials segregated from *Streptomyces aureofaciens* are called tetracycline antibiotics (TCs). Tetracycline prevents the growth of gram-positive and gram-negative bacteria,

\*Corresponding author.

Chlamydia, Mycoplasma, Rickettsia and protozoa parasites. TCs are widely used for the treatment of animal diseases and agricultural fertilizers. And, incomplete metabolism in animals and humans keeps them in aqueous ambience [5,6]. Tetracycline has also been identified in soil, surface water, ground water and even in drinking water [7,8]. These residues affect the human health and aqueous ecosystem and even produce resistant bacteria [5]. Since most of TCs are poorly absorbed by humans and animals, only about 80–90% of their initial amount is metabolized and the rest enters the ambience [8]. Studies on monitoring of TCs in the environment indicate that low concentrations ( $\text{ng L}^{-1}$  and  $\text{mg L}^{-1}$ ) in treated water and higher concentrations (100–500  $\text{mg L}^{-1}$ ) were detected in hospital and pharmaceutical companies' sewage [8,9]. Metronidazole (MNZ) is also one of the most widely used medications to treat infection caused by protozoa anaerobic bacteria such as giardia and Trichomonas Vaginalis. Metronidazole accumulation in the body is carcinogenic and mutagenic, resulting in DNA damage in human lymphocytes, which finally leads to acute toxicity in aquatic organisms [1,7,10]. Because of its high solubility in water and according low degradability, its discharge into the environment should be limited [11,12]. Several methods like biological processes, filtration, coagulation and flocculation and precipitation, advanced oxidation processes (AOPs), membrane filtration, absorption and combined systems have been applied for the removal of antibiotics from aqueous media. Each of these methods have different efficiencies, investment costs, interest rates, and advantages and disadvantages [13]. Absorption is one of the most effective methods for removing pollutants from aqueous solutions; further, it is easy to control and low cost. Different materials such as resin, activated carbon and nanocarbon are used for antibiotic adsorption. These substances can effectively eliminate antibiotics from water solutions [9]. Biochar is a convenient and affordable alternative to activated carbon for the removal of various pollutants from aqueous environments; it is prepared from different raw materials via the pyrolysis process. Also, its preparation needs low energy against activated carbon.

Type of raw material, temperature, and pyrolysis process used can effect on the quality and cost-effectiveness of biochar. Biochar is widely used to remove heavy metals, antibiotics and toxins from contaminated soils and water ambiances [14,15]. It's found that biochar has a high absorption capacity for organic and inorganic pollutants that it can be used for soil and water decontamination [16]. For example, rice bran is an adsorbent, which can be used for the removal of various pollutants like floroquinolone [17], ammonium nitrogen [18], dyes [19], heavy metals [20]. Removal of tetracycline and metronidazole has been performed by various materials, as an adsorbent, including carbon derived from the human hair [21], graphene oxide [22], fertilizer [23], activated carbon [7], multi-walled carbon nanotubes [24], biochar extracted from sugar bagasse [25], granular activated carbon [26], activated carbon obtained from the remaining coffee and almond shell [27]. Although few studies have been conducted on the mechanisms for the removal of tetracycline and metronidazole from aqueous media by biochar, the purpose of this study was to evaluate biochar potential as an adsorbent for the removal of tetracycline and metronidazole from aqueous media. The

batch tests and mathematical equations were used to determine the mechanism and characteristics of tetracycline and metronidazole adsorption on biochar. The special objectives included: 1) development of a simple and easy way to prepare cheap adsorbents to remove tetracycline and metronidazole, 2) evaluation of the ability to remove tetracycline and metronidazole and biochar mechanisms and 3) study of the effect of initial pH of the solution, contact time, initial tetracycline and metronidazole concentration and test temperature on the absorption of the antibiotics on biochar. The structure of TCs and MNZ has been shown in Table 1.

## 2. Materials and methods

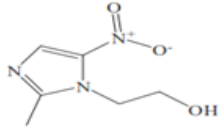
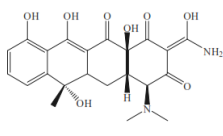
### 2.1. Chemicals

All of the materials used in this study were of a laboratory grade purchased from Merck Company without any purification. All solutions were prepared with de-ionized water. Biochar was prepared by the pyrolysis process from rice bran at 700°C in the absence of air. The rice bran was fragmented by a blender, sieved to a particle size of about 40–60 mesh and then dried at a temperature of 110°C for 8 h until complete removal of moisture in oven. It should be noted that rice bran is inexpensive and affordable.

### 2.2. Modification and characterization of biochar

Rice bran was collected from agricultural lands in northern Iran. In order to remove dust and impurities from the rice bran, it was washed several times with water. To increase its porosity, it was placed in 10% sulfuric acid on a shaker at room temperature for one hour and then washed with distilled water several times to reach neutral pH. Next, it was boiled in distilled water for one hour in a water bath (model Heidolph) and finally placed in an oven (model SHI-MAZCO) at 110°C for one night. After these stages, it was crushed again and sieved to the size of about 300  $\mu\text{m}$ . Biochar carbonization was performed inside a cylindrical furnace (AZAR FURNACES) under nitrogen gas (flow rate 0.1 l/min) with an increase in the temperature of from 10°C/min from room temperature to 80°C and then to 700°C for

Table 1  
Physicochemical characteristics and structure of TCs and MNZ

Molecular formula: $\text{C}_6\text{H}_9\text{N}_3\text{O}_3$	
Molar mass: 171.2 g/mol	
$P_{ka} = 2.55$	
Solubility: 9.5 g/l	
Molecular formula: $\text{C}_{22}\text{H}_{24}\text{N}_2\text{O}_8$	
Molar mass: 444.43 g/mol	
$P_{ka1} = 3.30$	
$P_{ka2} = 7.68$	
$P_{ka3} = 9.69$	
Solubility: 1.7 g/l	

2 h at a heating rate of 5°C/min. Afterwards, in order to room temperature it was kept in the furnace with nitrogen gas flow and finally stored as a powder until it was used inside the desiccator [28]. To explore the characteristics of the Biochar FT-IR ((Thermo-AVATAR-American) analysis Rice bran were performed at the range of 450–4000 cm<sup>-1</sup>. Morphology of the biochar surface was studied by a Stereo Scan S360 scanning electron microscope (SEM, MIRA3 TESCAN) operated at an accelerating voltage of 100 KV. The specific surface area was calculated by Brunauer–Emmett–Teller (BET) analysis (BELSORP MINI 2 Japan). Elemental analysis and chemical characterization of the biochar were conducted by Energy-dispersive X-ray spectroscopy (EDX).

### 2.3. Batch adsorption tests

In order to test the absorption of tetracycline and metronidazole on the biochar, the batch adsorption experiments were performed in 200-ml brown containers containing 100 ml of tetracycline and metronidazole solution separately at an initial concentration of 10–40 mg L<sup>-1</sup>. The containers' color was chosen in order to prevent the possible optical decomposition of tetracycline and metronidazole. The container was filled with antibiotic tetracycline and metronidazole solution at each stage, an appropriate amount of adsorbent was added to it and after adjusting pH on a shaker at 250 rpm and 298 K, the samples were taken after appropriate contact time and filtered with a pore size filter of 0.22 µm. So as to determine the concentration of antibiotics, TC and MNZ, HPLC, KNAUER- AZURA model with UV-Vis detectors at 358 and 319 nm wavelengths was used, respectively. The column temperature, sample injection rate and flow rate were 35°C, 20 µl, and 1 ml/min, respectively. For tetracycline, the moving phase of 0.01 M oxalic acid, ethanol and acetonitrile solutions were used at 70, 10, and 20 ratios, respectively [29,30]. Metronidazole moving phase including acetonitrile and distilled water with HPLC grade was used at 30–70 ratio, respectively [31,32]. The remaining concentrations of the antibiotics in solutions were determined through calculating the area under the curve. The concentrations of the standards prepared for drawing the standard curve were 0.25, 5.10, 15.20, 30 and 40 mg L<sup>-1</sup>. The regression coefficient R<sup>2</sup> after drawing the standard curve was higher than 0.99. The peak time of HPLC was 5.7 and 4.38 min for tetracycline and metronidazole, respectively. A series of absorption tests were performed to determine the solution pH, contact time, initial adsorbent concentration and initial antibiotic concentration. The removal efficiency of the antibiotics and their amounts during absorption and equilibrium were calculated by the following equations, respectively [3,13].

$$E(\%) = \frac{(C_0 - C_e)}{C_0} \times 100 \quad (1)$$

$$q_t = \frac{(C_0 - C_t) \times V}{m} \quad (2)$$

$$q_e = \frac{(C_0 - C_e) \times V}{m} \quad (3)$$

where  $E$  is the removal efficiency,  $C_0$  is the initial concentration of the antibiotics,  $C_t$  is the concentration of the antibiotics at any time,  $q_e$  is the absorption capacity at the equilibrium time,  $C_e$  is the equilibrium concentration of antibiotic solution,  $V$  (L) is the solution volume and  $m$  (g) is the absorbent mass.

### 2.4. Validity of isotherm and kinetic models

The application of kinetic and isotherm models was estimated by calculating normalized standard deviation (NSD), average relative error (ARE), marquardt's percentage standard deviation (MPSD) and hybrid error function (HYBRID) factors of model tests' data factors, and then used to predict the absorption behavior of tetracycline and metronidazole. The mathematical calculations of NSD, ARE, MPSD and HYBRID are presented below.

$$NSD\% = 100 \sqrt{\frac{1}{N-1} \sum_i^N \left[ \frac{q_{i,exp} - q_{i,cal}}{q_{i,exp}} \right]^2} \quad (4)$$

$$ARE = \frac{100}{N} \sum_{i=1}^n \left| \frac{q_{i,exp} - q_{i,cal}}{q_{i,exp}} \right| \quad (5)$$

$$MPSD = \sqrt{\frac{1}{N-p} \sum_i^N \left( \frac{q_{i,exp} - q_{i,cal}}{q_{i,exp}} \right)^2} \quad (6)$$

$$HYBRID = \frac{100}{N-p} \sum_{i=1}^n \left[ \frac{(q_{i,exp} - q_{i,cal})^2}{q_{i,exp}} \right] \quad (7)$$

where  $q_{i,exp}$  and  $q_{i,cal}$  (mg/g) are the experimental and calculated equilibrium of tetracycline and metronidazole adsorbed by biochar at any time  $t$ ,  $n$  is the number of tests, and  $p$  is the number of parameters in the regression model. The lower NSD, ARE, MPSD, and HYBRID values represents a more accurate estimate. Determination of isotherm and kinetics in addition to R<sup>2</sup>, the numerical values of NSD, ARE, MPSD and HYBRID also determine the number of parameters [28].

## 3. Results and discussion

### 3.1. Modified biochar characteristics

Table 2 and Fig. 1 present a list of ingredients and basic features of the biochar used in this study. As shown, the percentages of carbon and oxygen are 57.13% and 25.28%, respectively. These results are consistent with the those reported by Yi et al. and Sun et al. [17,33]. Since the raw material, from which the biochar is derived contains silica, the produced biochar is comprised of as much as 12.98% of silica [17]. The surface area of the biochar was 460.98 m<sup>2</sup>/g, which is more than that reported by similar studies. For example, Yi et al., Liu et al. and Liu et al. claimed that surface area and carbon percentage were 162 m<sup>2</sup>/g, 51.8% and 139.8 m<sup>2</sup>/g, 54.9% and 117.8 m<sup>2</sup>/g 76.4%, respectively [6,17,34–36]. It should be pointed out that the surface area is

Table 2  
Basic properties of the biochar

pH <sub>zpc</sub>	BTE (m <sup>2</sup> /g)	C BTE value	Total pore volume (cm <sup>3</sup> /g)	Mean pore diameter (nm)	Elemental composition (wt %)				
					C	N	O	Si	S
5.52	460.96	2019.8	0.2844	2.4677	57.13	1.18	25.28	12.98	0.19

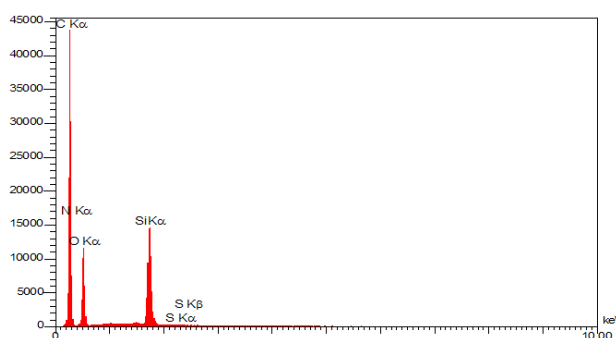


Fig. 1. EDX analyze of the biochar.

one of the important features showing the absorption capability of an adsorbent. A larger surface area illustrates the porous structure of biochar [17].

The results of the BET analysis have been summarized in Table 2. Based on the IUPAC classification, diameters less than 2 nm are micro porous, between 2 to 50 nm are meso porous and larger than 50 nm are macro porous [17]. The total pore volume at  $p/p_0 = 0.99$  by BET and BJH is 4.87 cc/g and 3.7 cc/g [14,17].

The findings showed that biochar pH<sub>zpc</sub> was 5.52. Biochar morphology was detected by FT-IR analysis in the range of 400–4000 cm<sup>-1</sup>, before and after absorption of tetracycline and metronidazole have been shown in Fig. 2. Based on the FT-IR analysis (Fig. 2), the position change of the band from the functional group has been shown in Fig. 2. Biochar hydroxyl-OH group is at the wavenumber of 3418 cm<sup>-1</sup>. The peak is related to the C-C bond and C-O group at 1600 cm<sup>-1</sup> and 1755 cm<sup>-1</sup>. A peak in the short wavelength or less than 1100 cm<sup>-1</sup> corresponds to a Si-O-Si bond [17,37]. Also, the peaks at 1096 cm<sup>-1</sup>, 1097 cm<sup>-1</sup> and 1099 cm<sup>-1</sup> are probably attributed to C-O stretching [38]. Moreover, the peaks at 1097, 1096 and 1099 cm<sup>-1</sup> are probably related to C-O [39]. The functional group of -NO<sub>2</sub> in the compounds of metronidazole after adsorption at 1387 cm<sup>-1</sup> may form an asymmetric of -NO<sub>2</sub> functional group in the range of 1530–1630 cm<sup>-1</sup>. The peak at 1628 cm<sup>-1</sup> is related to -NO<sub>2</sub> [40]. Tetracycline compounds have a carbonyl group [41]. Therefore, in FT-IR analysis, after the adsorption process a peak at 1728 cm<sup>-1</sup> and 1621 cm<sup>-1</sup> could be related to carbonyl ketone and carbonyl amide groups [42].

The pH<sub>zpc</sub> adsorbent assay was used to determine the surface charge. Biochar pH<sub>zpc</sub> was determined by adjusting the pH of sodium chloride solution in the range of 2–12. Six containers of 50 ml of 0.01 M sodium chloride solution were prepared and the pH was adjusted between 2–12 and then 0.15 g of the biochar was added to each of the containers. The samples were filtered after 48 h on a shaker at room temperature. The pH of each sample was measured [43]. As can be seen, biochar pH<sub>zpc</sub> is 5.52 (Fig. 3).

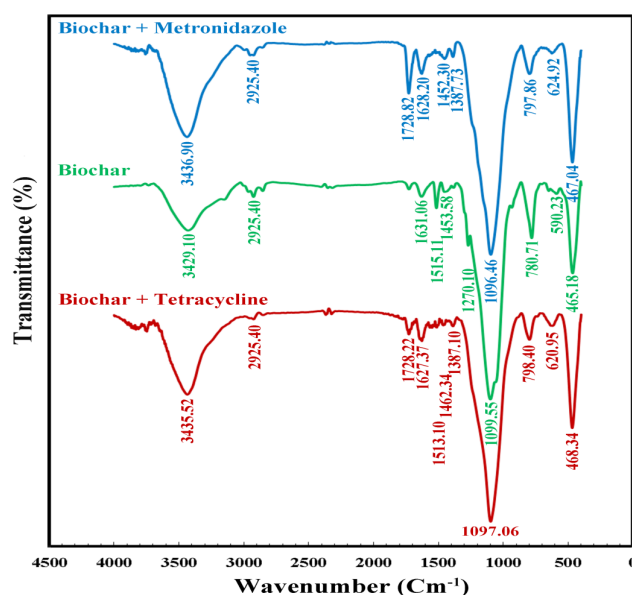


Fig. 2. The FT-IR spectrum of biochar sample before and after antibiotic adsorption.

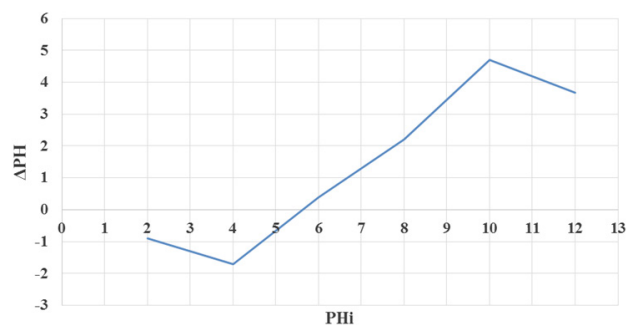


Fig. 3. Designation of pH in point of zero charge (PZC).

### 3.1.1. SEM analysis

Biochar level morphology was investigated by SEM image (Fig. 4). As shown, the rough surface of the activated carbon is visible, because most of the biochar is made of carbon. High porosity, which is a good feature for the adsorbent, is shown in this figure.

### 3.2. The effect of solution pH

The pH of the solution is one of the important factors in adsorption processes, because it affects the adsorbent surface charge and the type of adsorbent material

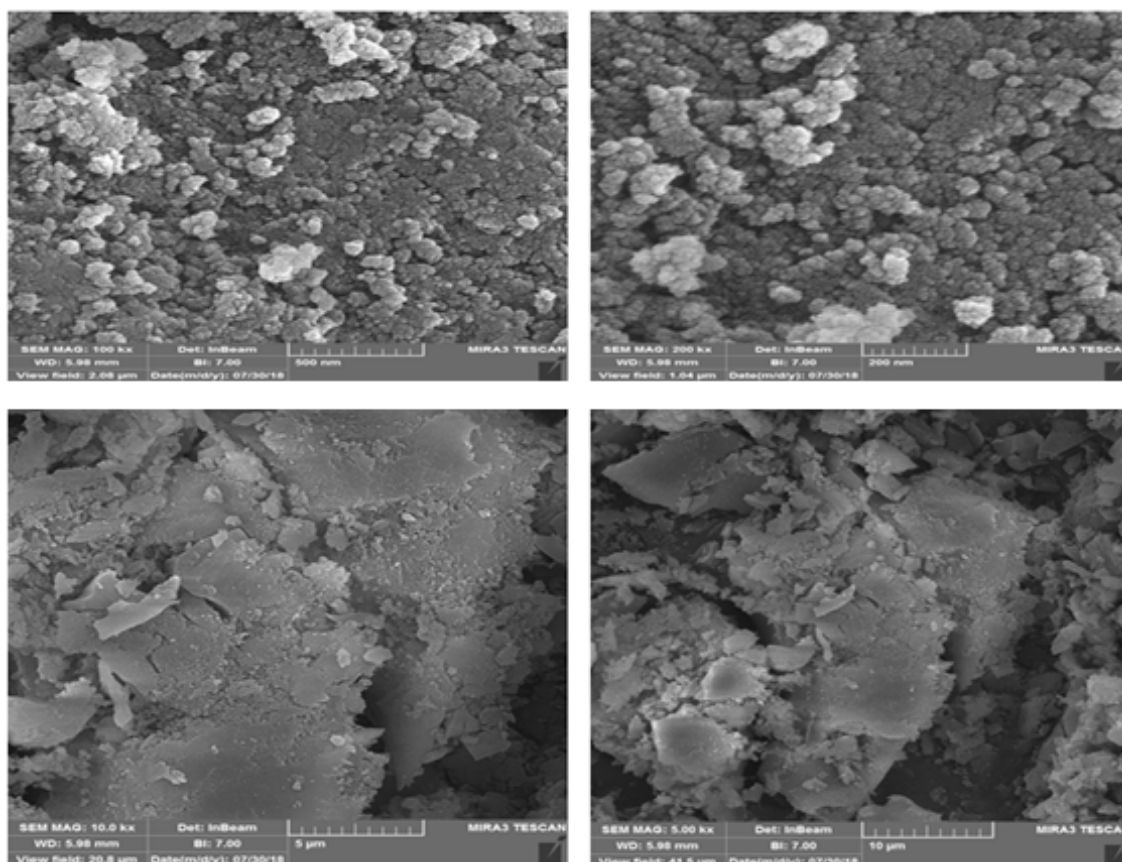


Fig. 4. SEM image of biochar sample.

and degree of ionization [44]. The effect of pH on the adsorption of tetracycline and metronidazole on the biochar was evaluated through an initial pH of 3–11 versus a constant concentration of antibiotic ( $10 \text{ mg L}^{-1}$ ) and a concentration of the adsorbent ( $1.5 \text{ g L}^{-1}$ ) (Fig. 5). As shown in Fig. 5, the removal efficiency of tetracycline and metronidazole increased by 3 to 5 (from 52% to 61% and 76% to 85%, respectively), and then it declined by 5 to 7% (from 61% to 50% and from 85% to 70%). The maximum adsorption capacity was attained at  $\text{pH} = 5$ . Biochar  $\text{pH}_{\text{zpc}}$  was also used to determine the surface charge. Biochar materials with amphoteric feature based on the solution pH can have a positive or negative surface. At  $\text{pH} > \text{pH}_{\text{zpc}}$ , biochar has a negative surface charge that adsorbs cationic material; by contrast, at  $\text{pH} < \text{pH}_{\text{zpc}}$ , biochar has a positive surface charge absorbing anionic compounds. In the present study, the biochar  $\text{pH}_{\text{zpc}}$  was found to be 5.52. Tetracycline is an amphoteric molecule with a multi-ionizing factor group, which may be cationic ( $\text{H}_3\text{L}^+$ ), dual charged ( $\text{H}_2\text{L}^0$ ) or anionic ( $\text{HL}^-$  and  $\text{L}^{2-}$ ). The distribution of tetracycline charge at different pHs depends on the type of  $\text{H}_3\text{L}^{+2}$  at  $\text{pH} < 3.4$ ,  $\text{HL}^-$  at  $3.4 < \text{pH} < 7.6$ ,  $\text{HL}^-$  at  $7.6 < \text{pH} < 9.0$  and  $\text{L}^{2-}$  at  $\text{pH} > 9.0$  (26). Based on tetracycline and adsorbent surface charge, the best adsorption pH in HL is  $3.4 < \text{pH} < 7.6$  in metronidazole antibiotics [26,33,45]. According to  $\text{pK}_a$ , which is 2.55 in most sources, its molecule in  $\text{pH} < \text{pK}_a$  has a positive charge and at  $\text{pH} > \text{pK}_a$  has a negative charge. Therefore,

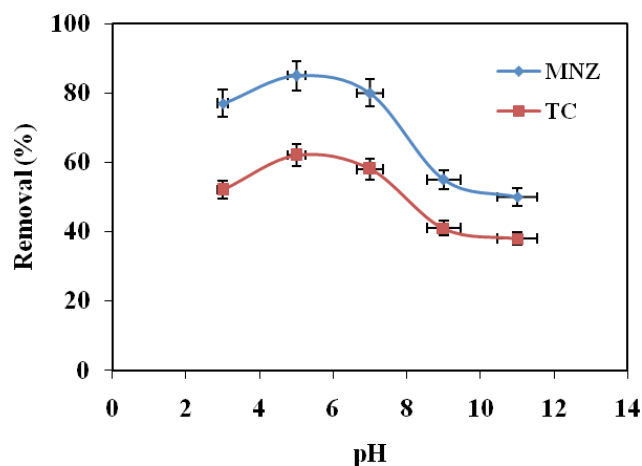


Fig. 5. Effect of solution pH on the adsorption of TC and MNZ onto the biochar (initial concentration:  $10 \text{ mg L}^{-1}$ , adsorbent dose:  $1.5 \text{ g L}^{-1}$ , contact time: 240 min).

at  $\text{pH} > \text{pH}_{\text{zpc}}$ , both biochar and metronidazole have a negative charge reducing adsorption. Therefore, the best adsorption state was attained at  $2.55 < \text{pH} < 5.52$ . In this study,  $\text{pH} = 5$  had the highest adsorption [26,46]. Similar results have been reported by Takdastan et al. and Chen et al. reporting that  $\text{pH} = 5$  was the best condition [6,13].

### 3.3. The effect of contact time

The contact time between the adsorbent and adsorbed is another important factor affecting the absorption efficiency. The data on the adsorption of tetracycline and metronidazole at initial concentrations of  $10 \text{ mg L}^{-1}$  with an adsorbent concentration of  $1.5 \text{ g L}^{-1}$  at  $\text{pH} = 5$  have been shown in Fig. 6. The results indicated that the adsorption capacity increased rapidly during the first 40 min, and then reduced to finally reach the equilibrium point at 120 min. The highest rate of adsorption at the early stages may be due to an increase in the number of vacant sites available on adsorbents, and no significant change was found in the adsorption rate between 90 and 120, which is due to the reduction in active sites available at biochar level. These results are consistent with other researchers' observations [47]. In the study of the adsorption of amoxicillin on activated carbon, the equilibrium time of 100 min was reported; also, in another study by Caliskan et al. the equilibrium time was found to be 150 min for adsorption metronidazole on activated carbon [40,48]. The main reason for the high adsorption rate at the initial adsorption time is related to the large surface on the biochar, which can provide many active sites for the adsorption of tetracycline and metronidazole [49].

### 3.4. The effect of adsorbent dose and initial concentrations of tetracycline and metronidazole

The adsorbent dose is also an important parameter in determining adsorption capacity. Fig. 7 shows the effect of the adsorbent dose and initial tetracycline and metronidazole concentrations on the adsorption of these antibiotics by the biochar under the optimum conditions ( $\text{pH} = 5$  and  $t = 120 \text{ min}$ ). According to Fig. 7, the efficiency increased with increasing the adsorbent dose from  $0.25 \text{ g L}^{-1}$  to  $1.5 \text{ g L}^{-1}$ . The results indicated that an increase in the adsorbent dose increased the active sites available on biochar special surface. Although an excessive increase in adsorbent dose

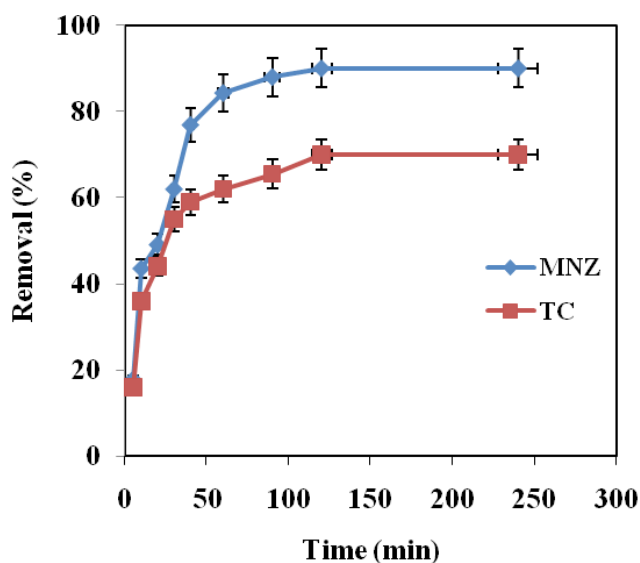


Fig. 6. The effect of contact time on TC and MNZ removal by biochar (initial concentration  $10 \text{ mg L}^{-1}$ , adsorbent dose =  $1.5 \text{ g L}^{-1}$ ,  $\text{pH} = 5$ ).

causes the accumulation and overlap of the active sites, this phenomenon reduces the access to active sites on the adsorbing surface and, in turn, absorption capacity reduction [50]. In the study by Chen et al., tetracycline adsorption onto rice husk ash, it was reported that the adsorbent dose  $2 \text{ g L}^{-1}$  was the optimum condition [6]. Also, in the study by Yi et al., levofloxacin adsorption onto rice husk biochar, the adsorbent dose of  $4 \text{ g L}^{-1}$  was the optimum condition [17].

Fig. 8 also shows that with increasing the initial tetracycline and metronidazole concentrations from  $10 \text{ mg L}^{-1}$  to  $40 \text{ mg L}^{-1}$  at the constant and optimum dose  $1.5 \text{ g L}^{-1}$ , the efficiency reduced from 70% to 50% and from 88.3% to 80%, respectively. At the low concentration of the antibiotics, the ratio of adsorption active sites to the total antibiotic molecules in the soluble phase was higher; in this state, most of the antibiotic molecules are in contact with the biochar, removed from the soluble phase. Thus, the adsorption

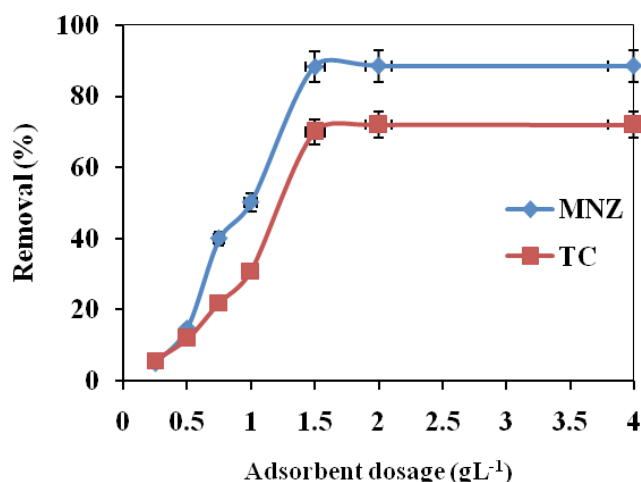


Fig. 7. The effect of adsorbent dose on TC and MNZ removal by biochar (initial TC and MNZ concentration =  $10 \text{ mg L}^{-1}$ , contact time = 120 min,  $\text{pH} = 5$ ).

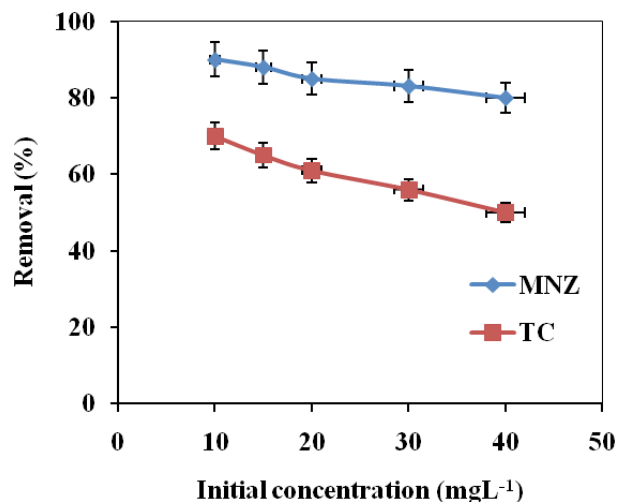


Fig. 8. The effect of initial TC and MNZ concentration on the removal efficiency by the biochar (adsorbent dose =  $1.5 \text{ g L}^{-1}$ , contact time = 120 min,  $\text{pH} = 5$ ).

Table 3  
The functional groups of the biochar sample defined by the FT-IR analysis

Functional group	Band positions (cm <sup>-1</sup> )
	Biochar
E O–H stretching	3429.10
Aliphatic C–H stretching	2925.40
Aromatic C–C stretching	1631.06
C–O stretching	1453.58
Si–O–Si asymmetric vibration	1099.55
Si–O–Si symmetrical	780.71
Stretching Si–O–Si flexural vibration	465.18

capacity increased with increasing initial antibiotic concentration. Because of the higher probability of collision between antibiotic and adsorbent molecules, the high concentration of antibiotics in the solution leads to a competition between antibiotic molecules in adsorption on sites, which gradually reduces absorption rate [45].

### 3.5. Equilibrium studies

The absorption isotherm is an equation that represents the absorbed transfer from the soluble phase to the adsorbent phase under equilibrium conditions. In order to obtain adsorption isotherms, 1.5 g L<sup>-1</sup> of the biochar was added to tetracycline and metronidazole solution with an antibiotic concentration 10 mg L<sup>-1</sup>–40 mg L<sup>-1</sup> with contact time of 4 h at pH = 5. In this study, nonlinear equations of Langmuir and Freundlich models were used in the Eqns. (8)–(10) to adapt the data of the experiments. These models are widely used to adapt the adsorption of various pollutants onto carbon-based adsorbents, such as active carbon [29,32,51].

$$\frac{C_e}{q_e} = \frac{1}{bQ_m} + \frac{C_e}{Q_m} \quad (8)$$

The Langmuir isotherm model adsorbs a single layer of adsorbed onto the adsorbent homogenous surface, which is its linear form.

$Q_m$  is the maximum amount of adsorption and  $b$  is the adsorption equilibrium constant [14,52].

$$R_L = \frac{1}{(1 + bC_0)} \quad (9)$$

$$\log q_e = \log K_f + \frac{1}{n} \log C_e \quad (10)$$

$K_f$  and  $n$  indicate the adsorption capacity and intensity, respectively. The lower value  $n$  [ $0 < n < 1$ ] indicates the weak adsorption force that affects the adsorbent surface.

In isotherm studies, when the Freundlich constant,  $n$ , is greater than 1, it indicates desired absorption conditions. Regarding the values of NSD,  $R^2$  and ARE, it can be concluded that the Freundlich isotherm model is the best model for adsorption. Tetracycline and metronidazole adsorption data showed that adsorption was heterogeneous on the biochar. The maximum adsorption capacity for tetracycline

Table 4  
The adsorption isotherm parameters for TC and MNZ adsorption onto the biochar

Antibiotic	Isotherm models	Parameters		
Tetracycline	Langmuir	$q_{e, exp}$	13.33	
		$q_m$ (mg g <sup>-1</sup> )	19.49	
		$b$ (L mg <sup>-1</sup> )	0.15	
		$R_L$	0.5	
		$R^2$	0.98	
		NSD	5.35	
		ARE	3.73	
		MPSD	0.6180	
		HYBRID	2.7	
		Freundlich	$K_f$ (mg g <sup>-1</sup> )	2.83
			$n$ (mg <sup>1-1/n</sup> g <sup>-1</sup> L <sup>1/n</sup> )	1.90
			$R^2$	0.99
			NSD	0.365
			ARE	2.82
MPSD	0.04214			
Metronidazole	Langmuir	$q_{e, exp}$	21.33	
		$q_m$ (mg g <sup>-1</sup> )	35.71	
		$b$ (L mg <sup>-1</sup> )	0.182	
		$R_L$	0.354	
		$R^2$	0.97	
		NSD	5.62	
		ARE	3.096	
		MPSD	0.0650	
		HYBRID	4.97	
		Freundlich	$K_f$ (mg g <sup>-1</sup> )	5.82
			$n$ (mg <sup>1-1/n</sup> g <sup>-1</sup> L <sup>1/n</sup> )	1.58
			$R^2$	0.99
			NSD	2.88
			ARE	1.94
MPSD	0.0334			
Freundlich	Freundlich	HYBRID	1.04	

and metronidazole were 13.33 and 21.33 mg/g, respectively. Compared with similar studies, for example, the results reported by Chen et al., tetracycline adsorption onto rice husk ash maximum absorption capacity was 8.37 mg/g [6]. In study by Sun et al., it was reported that maximum capacity was 21.61 mg/g for metronidazole adsorption onto biochar [25]. In another study by Azarpira et al., the maximum capacity was 31.2 mg/g for adsorption of metronidazole onto rice husk and Balarak et al., claimed maximum absorption capacity 24.9 mg/g for tetracycline on maize stalks [53–55].

### 3.6. Kinetic studies of absorption

Adsorption kinetics is one of the important data for understanding the mechanism of adsorption and evalu-

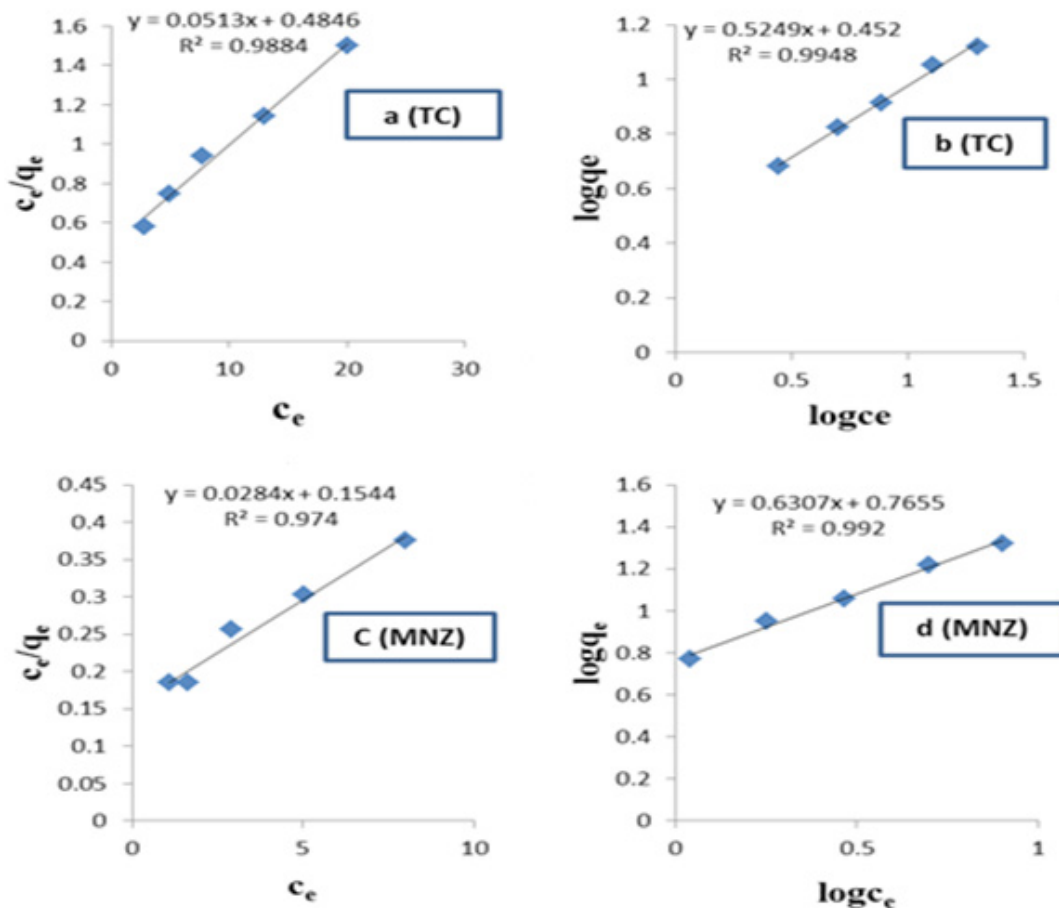


Fig. 9. The plots of (a) Langmuir isotherm for TC (b) Freundlich isotherm for TC and (c) Langmuir isotherm for MNZ (d) Freundlich isotherm for MNZ adsorption onto the biochar (initial TC and MNZ concentration = 10–40 mg L<sup>-1</sup>, adsorbent dose = 1.5g L<sup>-1</sup>, contact time = 24 h, pH = 5).

ation of process performance. In order to investigate the mechanism of tetracycline and metronidazole adsorption, we used a pseudo-first and second kinetics model to find the best model. The pseudo-first-order model is as follows [13,57]:

$$\ln(q_e - q_t) = \ln q_e - K_1 t \quad (11)$$

where,  $q_t$  and  $q_e$  are, respectively, the amount of tetracycline and metronidazole adsorbed at time  $t$  and equilibrium (mg/g) and  $k_1$  is the constant for the pseudo-first-order reaction. The pseudo-second-order equation is as follows:

$$\frac{t}{q_t} = \frac{1}{K_2 q_e^2} + \frac{1}{q_e} t \quad (12)$$

$K_2$  is fixed rate for the pseudo second order [32,58].

Table 6 shows correlation efficient  $R^2$ , NSD, ARE, MPSD, and HYBRID and fixed kinetic model for tetracycline and metronidazole adsorption on the biochar at the initial constant concentration 40 mg/L of tetracycline and metronidazole. The low correlation coefficient ( $<0.96$ ), NSD = 82.81, ARE = 59.82, MPSD = 0.82 and HYBRID = 914.17, pseudo first-order, high correlation coefficients ( $>0.99$ ), NSD = 11.86, ARE = 9.97, MPSD = 0.11 and HYBRID = 19.76

pseudo second order for tetracycline, low correlation coefficient ( $<0.94$ ), NSD = 12.38, ARE = 10, MPSD = 0.1242 and HYBRID = 914.17, pseudo first-order, ( $>0.99$ ), NSD = 6.82, ARE = 4.78, MPSD = 0.068 and HYBRID = 15.40 in pseudo second order, for metronidazole, confirms that pseudo first-order model did not have a good regression [46,49]. The results indicated that tetracycline and metronidazole adsorption followed the second order kinetic model. The value of  $q_e$  in the first-order kinetic model is not consistent with the experimental data. But the calculation of  $q_e$  with the pseudo-second-order kinetic model is fully consistent with the experimental data. The results illustrated that both antibiotics had the same reaction rate. The intra-particle diffusion model was applied for the kinetic data. This model can be defined by Eq. (13).

$$q_t = k_p \cdot t^{0.5} + c \quad (13)$$

where  $k$  is the intra-particle diffusion rate constant and  $C$  is the boundary layer thickness. A linear plot of  $q_t$  versus  $t^{1/2}$  at different initial concentrations has been shown in Fig. 9. The model parameters have been given in Table 5. As can be seen from Fig. 10, the diffusion kinetic plots exhibited the three-stage linearity. It has a good linear correlation between



Table 5  
Adsorption capacity comparison of biochar prepared from rice bran with other adsorbents used for antibiotics from aqueous solutions

Adsorbent	Adsorbent	Adsorption capacity mg/g	Reference
Rice husk ash	Tetracycline	8.37	[6]
Rice husk ash	Metronidazole	21.61	[25]
Rice husk	Metronidazole	31.2	[55]
Maize stalks	tetracycline	24.9	[56]
Rice husk ash	Tetracycline	21.33	This study

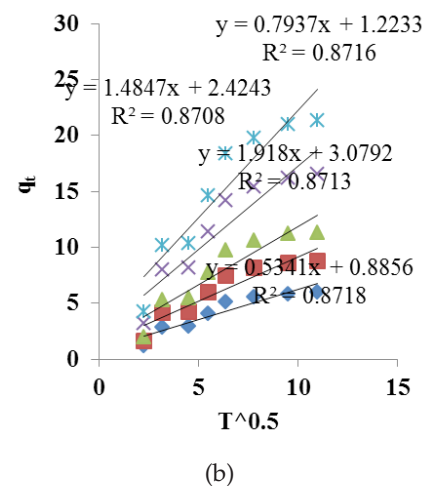
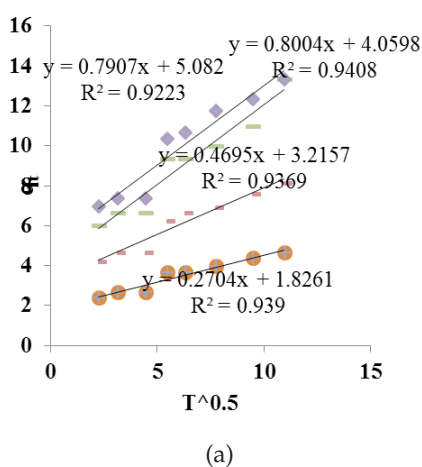


Fig. 10. Intra particle diffusion kinetic model for the adsorption of TC (a) and MNZ (b) adsorption onto the biochar.

$q_t$  and  $t^{1/2}$  in this stage, indicating that the adsorption process was not only controlled by intra-particle diffusion but two or more steps controlled the adsorption process.

3.7. Thermodynamics

We studied the effect of temperature on the absorption of tetracycline and metronidazole onto the biochar. The

Table 6  
Kinetic model parameters by the linear regression method for the adsorption of TC and MNZ by the biochar

Antibiotic	Kinetic models	Constants	
Tetracycline		$q_{e, exp}$	13.33
	Pseudo-first-order	$q_{e, cal}$	12.93
		$K_1$ (min <sup>-1</sup> )	0.026
		$R^2$	0.96
		NSD	82.81
		ARE	59.82
	Pseudo-second-order	MPSD	0.82
		HYBRID	914.17
		$q_{e, cal}$	14.43
		$K_2$ (min <sup>-1</sup> )	0.005
		$R^2$	0.99
	Intra-particle diffusion	NSD	11.86
		ARE	9.975
		MPSD	0.11
HYBRID		19.76	
C		10	
	$k_{id}$	0.80	
	$R^2$	0.9408	
Metronidazole		$q_{e, exp}$	21.33
	Pseudo-first-order	$q_{e, cal}$	21.28
		$K_1$ (min <sup>-1</sup> )	0.04
		$R^2$	0.94
		NSD	12.38
		ARE	10
	Pseudo-second-order	MPSD	0.1242
		HYBRID	52.39
		$q_{e, cal}$	22.76
		$K_2$ (min <sup>-1</sup> )	0.006
		$R^2$	0.99
	Intra-particle diffusion	NSD	6.82
		ARE	4.78
		MPSD	0.068
HYBRID		15.40	
C		10	
	$k_{id}$	0.7937	
	$R_2$	0.8718	

experiments were performed at 4 different temperatures (293, 298, 308, and 318°C) for two hours in a shaker-incubator (Heidolph Unimax 1010, Germany). The thermodynamic parameters consisting of the standard free energy change ( $\Delta G^0$ , kJ mol<sup>-1</sup>), enthalpy standard change ( $\Delta H^0$ , kJ mol<sup>-1</sup>) and entropy standard change ( $\Delta S^0$ , J mol<sup>-1</sup> K<sup>-1</sup>) were calculated to determine the absorption process. The values of  $\Delta G^0$ ,  $\Delta H^0$  and  $\Delta S^0$  were calculated by the following formulas:

$$\Delta G^0 = -RT \ln K_L \tag{14}$$

$$\ln K_L = \frac{\Delta S^\circ}{R} - \frac{\Delta H^\circ}{RT} \quad (15)$$

$$\ln K_L = \frac{q_e}{C_e} \quad (16)$$

$T$  is the temperature (K),  $R$  is the global gas constant, which is  $8.314 \text{ J mol}^{-1} \text{ K}^{-1}$ , and the constant  $K_L$  is Langmuir's isotherm in  $\text{L mg}^{-1}$ . The values of  $\Delta H^\circ$ ,  $\Delta S^\circ$ , and  $\Delta G^\circ$  are calculated according to the slope and y-intercept, respectively,  $\ln K_L$  curves vs.  $1/T$  and Eqs. (14)–(16).

Gibbs free energy changes ( $\Delta G$ ) are determined by both energy and entropy; the results of which indicate the spontaneous reaction and feasibility of the adsorption reaction. The negative value of  $\Delta G$  represents the spontaneous nature of the reaction at a given temperature [14]. In addition, the negative values of  $\Delta G$  increase with increasing temperature; that is, tetracycline and metronidazole adsorption was more desired at higher temperatures on the biochar.  $\Delta H$  can be used to identify the nature of the adsorbent. For example, a value in the range of 2.1–20.9 kJ/mol indicating the physical absorption [14]. Table 7 shows the values of the thermodynamic parameters. The free energy change of  $\Delta G$  for tetracycline and metronidazole adsorption process was  $-0.85$ ,  $-1.090$ ,  $-1.51$ ,  $-1.74$ ,  $-3.87$ ,  $-3.87$ ,  $-3.87$ , and  $-4.49$  kJ/mol at temperatures of 293, 298, 308, and 318°C, respectively. The results of  $\Delta G$  numbers indicate that the absorption process is desirable and spontaneous. According to the value of  $\Delta H$  in Table 7 (6.29 and 2.12 kJ/mol, respectively, for tetracycline and metronidazole), it can be concluded that the adsorption process was endothermic and more desired at higher temperatures [59,60]. Typically, the positive integer value  $\Delta S$  represent a significant increase at solid-solution level during absorption and a slight structural change in adsorbent and absorbed, resulting in irreversible reactions [6,7,46]. The results showed that the adsorption capacity was not very much affected by the temperature because the absorption isotherm overlapped at the studied temperatures [48,61].

#### 4. Conclusion

The biochar, with very good quality, was successfully prepared from rice bran as an adsorbent to remove tetracycline and metronidazole from aqueous ambience. The maximum efficacy rates of tetracycline and metronidazole in this survey was 70% and 90%, respectively. Metronidazole was removed more than tetracycline, due to its size (444.43, 171.2 g/mol) and electron density. The adsorption of tetra-

cycline and metronidazole followed a pseudo second order kinetics, and the adsorption equilibrium followed the Freundlich isotherm model. Tetracycline and metronidazole adsorption procedure on the biochar was spontaneous and endothermic. As a result, the biochar prepared from rice bran is an optimal adsorbent for tetracycline and metronidazole removal from aqueous solutions. Thus, this research could be a basic reference for future studies for the production of the advanced modification biochar to remove pollutants from environments.

#### Acknowledgements

The authors want to thank authorities of Iran University of Medical Sciences for their comprehensive support for this study.

#### Conflict of Interest

The authors of this article declare that they have no conflict of interests.

#### References

- [1] N. Okhovat, M. Hashemi, A. Golpayegani, Photocatalytic decomposition of Metronidazole in aqueous solutions using titanium dioxide nanoparticles, *J. Mater. Environ. Sci.*, 6 (2015) 792–799.
- [2] B. Kakavandi, A. Takdastan, N. Jaafarzadeh, M. Azizi, A. Mirzaei, A. Azari, Application of  $\text{Fe}_3\text{O}_4/\text{C}$  catalyzing heterogeneous UV-Fenton system for tetracycline removal with a focus on optimization by a response surface method, *J. Photochem. Photobiol. A: Chem.*, 314 (2016) 178–188.
- [3] B. Kakavandi, A. Esrafil, A. Mohseni-Bandpi, A.J. Jafari, R.R. Kalantary, Magnetic  $\text{Fe}_3\text{O}_4/\text{C}$  nanoparticles as adsorbents for removal of amoxicillin from aqueous solution, *Water Sci. Technol.*, 69 (2014) 147.
- [4] Y. Deng, L. Tang, G. Zeng, J. Wang, Y. Zhou, J. Wang, J. Tang, L. Wang, C. Feng, Facile fabrication of mediator-free Z-scheme photocatalyst of phosphorus-doped ultrathin graphitic carbon nitride nanosheets and bismuth vanadate composites with enhanced tetracycline degradation under visible light, *J. Colloid Interface Sci.*, 509 (2018) 219–234.
- [5] F. Yu, Y. Li, S. Han, J. Ma, Adsorptive removal of antibiotics from aqueous solution using carbon materials, *Chemosphere*, 153 (2016) 365–385.
- [6] Y. Chen, F. Wang, L. Duan, H. Yang, J. Gao, Tetracycline adsorption onto rice husk ash, an agricultural waste: its kinetic and thermodynamic studies, *J. Mol. Liq.*, 222 (2016) 487–494.
- [7] H. Belhassen, I. Ghorbel-Abid, L. Rim, Removal of metronidazole from aqueous solution using activated carbon, *Eur. J. Chem.*, 8 (2017) 310–313.
- [8] M. Ahmadi, H.R. Motlagh, N. Jaafarzadeh, A. Mostoufi, R. Saeedi, G. Barzegar, S. Jorfi, Enhanced photocatalytic degradation of tetracycline and real pharmaceutical wastewater using MWCNT/TiO<sub>2</sub> nano-composite, *J. Environ. Manage.*, 186 (2017) 55–63.
- [9] W. Khanday, B. Hameed, Zeolite-hydroxyapatite-activated oil palm ash composite for antibiotic tetracycline adsorption, *Fuel*, 215 (2018) 499–505.
- [10] A. Aboudalle, H. Djelal, F. Fourcade, L. Domergue, A.A. Assadi, T. Lendormi, S. Taha, A. Amrane, Metronidazole removal by means of a combined system coupling an electro-Fenton process and a conventional biological treatment: By-products monitoring and performance enhancement, *J. Hazard. Mater.*, 359 (2018) 85–95.

Table 7

Adsorption thermodynamic parameters for TC and MNZ adsorption on the biochar

Antibiotic	$\Delta S$ ( $\text{J mol}^{-1} \text{ K}^{-1}$ )	$\Delta H$ ( $\text{kJ mol}^{-1}$ )	$\Delta G$ ( $\text{kJ mol}^{-1}$ ) Temperature (K)			
			293	298	308	318
Tetracycline	0.025	6.29	-0.85	-1.090	-1.51	-1.74
Metronidazole	0.024	2.12	-3.87	-3.87	-3.87	-4.49

- [11] X. Bu, Y. Wang, J. Li, C. Zhang, Improving the visible light photocatalytic activity of TiO<sub>2</sub> by combining sulfur doping and rectorite carrier, *J. Alloys Comp.*, 628 (2015) 20–26.
- [12] N. Jafarzadeh, H. Rezazadeh, Z. Ramezani, S. Jorfi, M. Ahmadi, H. Ghariby, G. Barzegar, Taguchi optimization approach for metronidazole removal from aqueous solutions by using graphene oxide functionalized  $\beta$ -cyclodextrin/Ag nanocomposite, *Water Sci. Technol.*, 2017 (2018) 36–47.
- [13] A. Takdastan, A.H. Mahvi, E.C. Lima, M. Shirmardi, A.A. Babaei, G. Goudarzi, A. Neisi, M. Heidari Farsani, M. Vosoughi, Preparation, characterization, and application of activated carbon from low-cost material for the adsorption of tetracycline antibiotic from aqueous solutions, *Water Sci. Technol.*, 74 (2016) 2349–2363.
- [14] M. Vithanage, S. Mayakaduwa, I. Herath, Y.S. Ok, D. Mohan, Kinetics, thermodynamics and mechanistic studies of carbofuran removal using biochars from tea waste and rice husks, *Chemosphere*, 150 (2016) 781–789.
- [15] Y.-d. Huang, Comment on “Evaluation of the effectiveness and mechanisms of acetaminophen and methylene blue dye adsorption on activated biochar derived from municipal solid wastes”, *J. Environ. Manage.*, (2018).
- [16] H. Chen, A. Xie, S. You, A Review: Advances on Absorption of Heavy Metals in the Waste Water by Biochar, in: *IOP Conference Series: Materials Science and Engineering*, IOP Publishing, 2018, pp. 012160.
- [17] S. Yi, B. Gao, Y. Sun, J. Wu, X. Shi, B. Wu, X. Hu, Removal of levofloxacin from aqueous solution using rice-husk and wood-chip biochars, *Chemosphere*, 150 (2016) 694–701.
- [18] S. Kizito, S. Wu, W.K. Kirui, M. Lei, Q. Lu, H. Bah, R. Dong, Evaluation of slow pyrolyzed wood and rice husks biochar for adsorption of ammonium nitrogen from piggy manure anaerobic digestate slurry, *Sci. Total Environ.*, 505 (2015) 102–112.
- [19] S. Dawood, T.K. Sen, C. Phan, Performance and dynamic modelling of biochar and kaolin packed bed adsorption column for aqueous phase methylene blue (MB) dye removal, *Environ. Technol.*, (2018) 1–35.
- [20] E.-B. Son, K.-M. Poo, J.-S. Chang, K.-J. Chae, Heavy metal removal from aqueous solutions using engineered magnetic biochars derived from waste marine macro-algal biomass, *Sci. Total Environ.*, 615 (2018) 161–168.
- [21] M. Ahmed, M.A. Islam, M. Asif, B. Hameed, Human hair-derived high surface area porous carbon material for the adsorption isotherm and kinetics of tetracycline antibiotics, *Bioresour. Technol.*, 243 (2017) 778–784.
- [22] L. He, F.-f. Liu, M. Zhao, Z. Qi, X. Sun, M.Z. Afzal, X. Sun, Y. Li, J. Hao, S. Wang, Electronic-property dependent interactions between tetracycline and graphene nanomaterials in aqueous solution, *J. Environ. Sci.*, 66 (2018) 286–294.
- [23] T. Chen, L. Luo, S. Deng, G. Shi, S. Zhang, Y. Zhang, O. Deng, L. Wang, J. Zhang, L. Wei, Sorption of tetracycline on H<sub>3</sub>PO<sub>4</sub> modified biochar derived from rice straw and swine manure, *Bioresour. Technol.*, 267 (2018) 431–437.
- [24] S.A. Mousavi, H. Janjani, Antibiotics adsorption from aqueous solutions using carbon nanotubes: a systematic review, *Toxin Rev.*, (2018) 1–12.
- [25] L. Sun, D. Chen, S. Wan, Z. Yu, Adsorption studies of dimetridazole and metronidazole onto biochar derived from sugarcane bagasse: kinetic, equilibrium, and mechanisms, *J. Polym. Environ.*, 26 (2018) 765–777.
- [26] P. Liu, Q. Wang, C. Zheng, C. He, Sorption of sulfadiazine, norfloxacin, metronidazole, and tetracycline by granular activated carbon: kinetics, mechanisms, and isotherms, *Water Air Soil Pollut.*, 228 (2017) 129.
- [27] J. Flores-Cano, M. Sánchez-Polo, J. Messoud, I. Velo-Gala, R. Ocampo-Pérez, J. Rivera-Utrilla, Overall adsorption rate of metronidazole, dimetridazole and diatrizoate on activated carbons prepared from coffee residues and almond shells, *J. Environ. Manage.*, 169 (2016) 116–125.
- [28] A. Gholizadeh, M. Kermani, M. Gholami, M. Farzadkia, Kinetic and isotherm studies of adsorption and biosorption processes in the removal of phenolic compounds from aqueous solutions: comparative study, *J. Environ. Health Sci. Eng.*, 11 (2013) 29.
- [29] A.A. Babaei, E.C. Lima, A. Takdastan, N. Alavi, G. Goudarzi, M. Vosoughi, G. Hassani, M. Shirmardi, Removal of tetracycline antibiotic from contaminated water media by multi-walled carbon nanotubes: operational variables, kinetics, and equilibrium studies, *Water Sci. Technol.*, 74 (2016) 1202–1216.
- [30] Y. Liu, J. Kong, J. Yuan, W. Zhao, X. Zhu, C. Sun, J. Xie, Enhanced photocatalytic activity over flower-like sphere Ag/Ag<sub>2</sub>CO<sub>3</sub>/BiVO<sub>4</sub> plasmonic heterojunction photocatalyst for tetracycline degradation, *Chem. Eng. J.*, 331 (2018) 242–254.
- [31] M. Farzadkia, E. Bazrafshan, A. Esrafil, J.-K. Yang, M. Shirzad-Siboni, Photocatalytic degradation of Metronidazole with illuminated TiO<sub>2</sub> nanoparticles, *J. Environ. Health Sci. Eng.*, 13 (2015) 35.
- [32] A. Habibi, L.S. Belaroui, A. Bengueddach, A.L. Galindo, C.I.S. Díaz, A. Peña, Adsorption of metronidazole and spiramycin by an Algerian palygorskite. Effect of modification with tin, *Micropor. Mesopor. Mater.*, 268 (2018) 293–302.
- [33] Y. Sun, B. Gao, Y. Yao, J. Fang, M. Zhang, Y. Zhou, H. Chen, L. Yang, Effects of feedstock type, production method, and pyrolysis temperature on biochar and hydrochar properties, *C Chem. Eng. J.*, 240 (2014) 574–578.
- [34] X.-R. Jing, Y.-Y. Wang, W.-J. Liu, Y.-K. Wang, H. Jiang, Enhanced adsorption performance of tetracycline in aqueous solutions by methanol-modified biochar, *Chem. Eng. J.*, 248 (2014) 168–174.
- [35] W.-J. Liu, F.-X. Zeng, H. Jiang, X.-S. Zhang, Preparation of high adsorption capacity bio-chars from waste biomass, *Bioresour. Technol.*, 102 (2011) 8247–8252.
- [36] P. Liu, W.-J. Liu, H. Jiang, J.-J. Chen, W.-W. Li, H.-Q. Yu, Modification of bio-char derived from fast pyrolysis of biomass and its application in removal of tetracycline from aqueous solution, *Bioresour. Technol.*, 121 (2012) 235–240.
- [37] M. Vieira, A. de Almeida Neto, M. Da Silva, C. Carneiro, A. Melo Filho, Adsorption of lead and copper ions from aqueous effluents on rice husk ash in a dynamic system, *Brazil. J. Chem. Eng.*, 31 (2014) 519–529.
- [38] D. Zhang, J. Yin, J. Zhao, H. Zhu, C. Wang, Adsorption and removal of tetracycline from water by petroleum coke-derived highly porous activated carbon, *J. Environ. Chem. Eng.*, 3 (2015) 1504–1512.
- [39] A.A. Mohammadi, A. Zarei, H. Alidadi, M. Afsharnia, M. Shams, Two-dimensional zeolitic imidazolate framework-8 for efficient removal of phosphate from water, process modeling, optimization, kinetic, and isotherm studies, *Desal. Water Treat.*, 129 (2018) 244–254.
- [40] E. Çalıřkan, S. Göktürk, Adsorption characteristics of sulfamethoxazole and metronidazole on activated carbon, *Separ. Sci. Technol.*, 45 (2010) 244–255.
- [41] J. Kang, H. Liu, Y.-M. Zheng, J. Qu, J.P. Chen, Application of nuclear magnetic resonance spectroscopy, Fourier transform infrared spectroscopy, UV-Visible spectroscopy and kinetic modeling for elucidation of adsorption chemistry in uptake of tetracycline by zeolite beta, *J. Colloid Interface Sci.*, 354 (2011) 261–267.
- [42] L. Zhang, X. Song, X. Liu, L. Yang, F. Pan, J. Lv, Studies on the removal of tetracycline by multi-walled carbon nanotubes, *Chem. Eng. J.*, 178 (2011) 26–33.
- [43] J. He, P. Ma, A. Xie, L. Gao, Z. Zhou, Y. Yan, J. Dai, C. Li, From black liquor to highly porous carbon adsorbents with tunable microstructure and excellent adsorption of tetracycline from water: performance and mechanism study, *J. Taiwan Inst. Chem. Eng.*, 63 (2016) 295–302.
- [44] E. Zong, G. Huang, X. Liu, W. Lei, S. Jiang, Z. Ma, J. Wang, P. Song, A lignin-based nano-adsorbent for superfast and highly selective removal of phosphate, *J. Mater. Chem. A*, 6 (2018) 9971–9983.
- [45] M.M. Ali, M. Ahmed, B. Hameed, NaY zeolite from wheat (*Triticum aestivum* L.) straw ash used for the adsorption of tetracycline, *J. Cleaner Prod.*, 172 (2018) 602–608.
- [46] E. Yeřilova, B. Osman, A. Kara, E.T. Özer, Molecularly imprinted particle embedded composite cryogel for selective tetracycline adsorption, *Separ. Purif. Technol.*, 200 (2018) 155–163.

- [47] D. Balarak, F.K. Mostafapour, Canola residual as a biosorbent for antibiotic metronidazole removal, *Pharm. Chem. J.*, 3 (2016) 12–17.
- [48] H. Saygılı, F. Güzel, Effective removal of tetracycline from aqueous solution using activated carbon prepared from tomato (*Lycopersicon esculentum* Mill.) industrial processing waste, *Ecotoxicol. Environ. Safety*, 131 (2016) 22–29.
- [49] A. Gholizadeh, M. Kermani, M. Gholami, M. Farzadkia, K. Yaghmaeian, Removal efficiency, adsorption kinetics and isotherms of phenolic compounds from aqueous solution using rice bran ash, *Asian J. Chem.*, 25 (2013) 3871.
- [50] R.R. Kalantary, A. Azari, A. Esrafil, K. Yaghmaeian, M. Moradi, K. Sharafi, The survey of Malathion removal using magnetic graphene oxide nanocomposite as a novel adsorbent: thermodynamics, isotherms, and kinetic study, *Desal. Water Treat.*, 57 (2016) 28460–28473.
- [51] S. Ahmadi, A. Banach, F. Kord Mostafapour, D. Balarak, Study survey of cupric oxide nanoparticles in removal efficiency of ciprofloxacin antibiotic from aqueous solution: adsorption isotherm study, *Desal. Water Treat.*, 89 (2017) 297–303.
- [52] M.H. Dehghani, S. Kamalian, M. Shayeghi, M. Yousefi, Z. Heidarinejad, S. Agarwal, V.K. Gupta, High-performance removal of diazinon pesticide from water using multi-walled carbon nanotubes, *Microchem. J.*, 145 (2019) 486–491.
- [53] D. Balarak, H. Azarpira, F. Mostafapour, Adsorption isotherm studies of tetracycline antibiotics from aqueous solutions by maize stalks as a cheap biosorbent, *Int. J. Pharm. Technol.*, 8 (2016) 16664–16675.
- [54] D. Balarak, H. Azarpira, Rice husk as a Biosorbent for antibiotic metronidazole removal: Isotherm studies and model validation, *Int. J. ChemTech Res.*, 9 (2016) 566–573.
- [55] H. Azarpira, D. Balarak, Rice husk as a biosorbent for antibiotic metronidazole removal: Isotherm studies and model validation, *Int. J. ChemTech Res.*, 9 (2016) 566–573.
- [56] D. Balarak, F. Mostafapour, H. Azarpira, Adsorption isotherm studies of tetracycline antibiotics from aqueous solutions by maize stalks as a cheap biosorbent, *Int. J. Pharm. Technol.*, 8 (2016) 16664–16675.
- [57] S. Mazloomi, M. Yousefi, H. Nourmoradi, M. Shams, Evaluation of phosphate removal from aqueous solution using metal organic framework; isotherm, kinetic and thermodynamic study, *J. Environ. Health Sci. Eng.*, (2019) 1–10.
- [58] H.N. Saleh, M.H. Dehghani, R. Nabizadeh, A.H. Mahvi, F. Hossein, M. Ghaderpoori, M. Yousefi, A. Mohammadi, Data on the acid black 1 dye adsorption from aqueous solutions by low-cost adsorbent-*Cerastoderma lamarcki* shell collected from the northern coast of Caspian Sea, *Data in Brief*, 17 (2018) 774–780.
- [59] M.N. Sepehr, T.J. Al-Musawi, E. Ghahramani, H. Kazemian, M. Zarrabi, Adsorption performance of magnesium/aluminum layered double hydroxide nanoparticles for metronidazole from aqueous solution, *Arabian J. Chem.*, 10 (2017) 611–623.
- [60] H. Azarpira, Y. Mahdavi, O. Khaleghi, D. Balarak, Thermodynamic studies on the removal of metronidazole antibiotic by multi-walled carbon nanotubes, *Der Pharmacia Lettre*, 8 (2016) 107–113.
- [61] D. Carrales-Alvarado, R. Ocampo-Pérez, R. Leyva-Ramos, J. Rivera-Utrilla, Removal of the antibiotic metronidazole by adsorption on various carbon materials from aqueous phase, *J. Colloid Interface Sci.*, 436 (2014) 276–285.